

Electronic and geometric structure of NH₃ on Ge(001) under equilibrium adsorption conditions

W. Ranke and J. Platen

Fritz-Haber-Institut der Max-Planck-Gesellschaft, Faradayweg 4-6, D-14195 Berlin (Dahlem), Germany

(Received 13 November 1995)

The adsorption of NH₃ on the Ge(001) surface is studied by angle-resolved UV-photoelectron spectroscopy using synchrotron radiation and by high-resolution low-energy electron diffraction (LEED) measurements. On the clean surface, the phase transition from 2×1 to c(4×2) is observed over a temperature range from 400 to 220 K. Measurements during NH₃ admission at varying temperature in adsorption-desorption equilibrium yield a sequential occupation of several states. Up to ½ ML (one molecule per reconstruction dimer), NH₃ is bound strongly on the dimer down atoms with the Ge-N axis perpendicular to the surface (α state). The adsorption occurs via a mobile precursor state. The α state is connected with a (2×2) superstructure. Yet, the transition c(4×2)→(2×2) starts already at very low coverages (0.01 ML) and is completed for about 0.04 ML. We propose that a long-range attractive interaction causes α -NH₃-island formation and that a short-range repulsive interaction is responsible for a change to 2×2 within the islands by a dimer flip of every second dimer row. At the island edges, this dimer flip continues over the clean part of the surface thus changing its structure to 2×2 long before ½ ML saturation. Beyond ½ ML, the structure changes again. A good-quality 2×1 structure is seen up to 4 ML indicating pseudomorphic growth up to this coverage. Beyond 4 ML, the adsorbate structure changes irreversibly to NH₃-ice without any LEED pattern. [S0163-1829(96)08227-6]

I. INTRODUCTION

Similar to the Si(001) surface, Ge(001) reconstructs by forming asymmetric dimers.¹⁻⁴ Different from Si, however, ammonia adsorbs molecularly on Ge surfaces.⁵⁻⁷ The interaction with the surface is not so strong that the molecular structure of the adsorbate is severely affected or that substrate bonds are broken but it is strong enough to be sensitive to the geometry and electronic properties of different sites. It is thus an interesting model system. In a recent study,⁸ we have investigated the adsorption-desorption equilibrium in the temperature range 90–400 K at pressures below 10⁻⁶ mbar. The intensity of the NH₃-1*e* orbital in photoelectron spectra excited with 21.2 eV was used as a measure of the coverage. From its variation with temperature and pressure, isosteric heats of adsorption $\Delta H_{\text{ad}}(\Theta)$ were deduced for several surface orientations, including (001), (113), and (111). Adsorption on (001) turned out to be especially exciting. Up to a coverage of ½ ML (i.e., one molecule per reconstruction dimer, α state), $\Delta H_{\text{ad}}(\Theta)$ is high and increases with coverage from about 90 to 135 kJ/mol which was attributed to an attractive interaction between the adsorbed molecules. The work function decreases linearly with coverage by as much as 2.1 eV. After saturation of this state, $\Delta H_{\text{ad}}(\Theta)$ drops to an almost constant value of 40–45 kJ/mol until 2 ML (β_1 state), followed by a further drop to 32 kJ/mol up to 4 ML (β_2 state). Compared to the first half ML, the further work-function drop is small and amounts to additional 0.4 eV. At about 1.3 ML, the layer transforms to a state with lower entropy, i.e., with higher order but within our experimental accuracy, this transition is not connected with a change of ΔH_{ad} or work function. Beyond 4 ML, an irreversible structural change of the layer occurs and normal condensation is observed (γ state).

In this paper, we concentrate on structural aspects of this adsorption sequence. In a previous paper,⁵ we have presented

evidence from selection rule arguments in photoemission that the strongly bound first half ML of NH₃ adsorbs perpendicularly. We have repeated these measurements under the better defined conditions of adsorption-desorption equilibrium. Further, high resolution low-energy electron diffraction (LEED) measurements including spot-profile analysis (SPALEED) are presented which show that the sequence of adsorption states is related with a sequence of changes in surface structure.

II. EXPERIMENT

Molecularly adsorbed NH₃ is sensitive to electron irradiation and to the secondary electrons produced during exposure to high-energy photons.⁵ Due to the very small focus of the used synchrotron radiation, satellites of the valence orbitals of NH₃ appeared already after a short time indicating decomposition, especially for coverages up to ½ ML (α state). Therefore, the sample was irradiated only for a few minutes on the same spot. He I radiation ($h\nu=21.2$ eV) is harmless. LEED measurements were made with a Henzler-type spot profile analysis system⁹ which uses very low electron doses on a relatively large spot. No influence was noticed.

Two stainless-steel chambers with a base pressure below 6×10⁻¹¹ mbar were used. One of them contained the SPALEED instrument and a double-pass cylindrical mirror analyzer for ultraviolet photoemission spectroscopy (UPS) using He I radiation, averaging over a large escape angle range. The second chamber contained an angle-resolving photoelectron spectrometer (ADES 400, Vacuum Generators) and a display LEED optics. It was connected to the toroidal grating monochromator TGM 4 beamline at the synchrotron source, Berliner Elektronenspeicherring-Gesellschaft für Synchrotronstrahlung m.b.H. (BESSY), in Berlin. Sample cleanliness and order could further be controlled by Auger

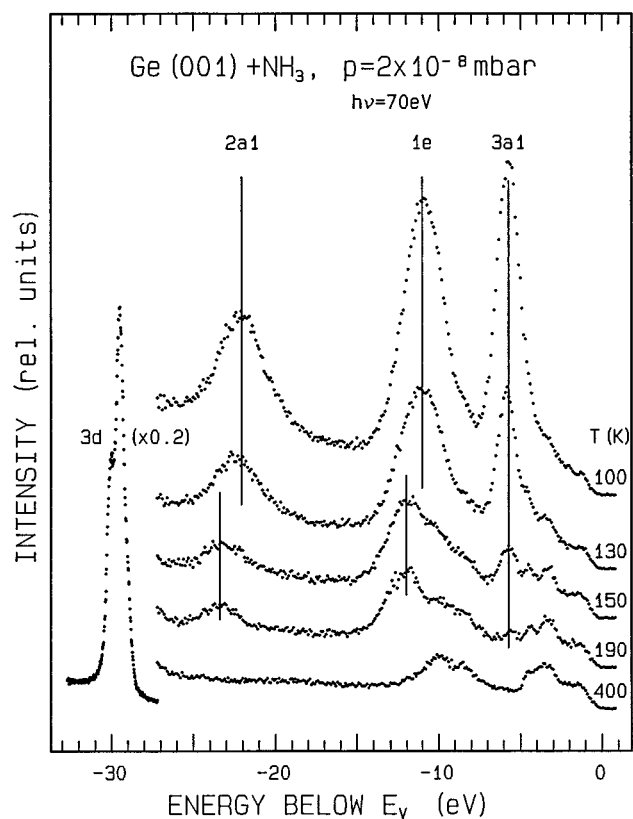


FIG. 1. Photoelectron spectra of Ge(001) under constant NH_3 pressure of 2×10^{-8} mbar, taken at different sample temperatures; incidence angle 45° , escape angle 60° with respect to the sample normal, $h\nu = 70$ eV. The NH_3 coverage (in ML) is approximately: clean at 400 K, 0.5 at 190 K, 0.65 at 150 K, 1.15 at 130 K, and 2 at 100 K.

electron spectroscopy. Ammonia was admitted via the residual gas. An influence of the ionization gauge was not noticed. Due to the long exposures and NH_3 condensation on the cold areas of the sample holder, which evaporated after warm-up, a pressure of about 2×10^{-10} mbar could only be achieved the following morning, if the chamber was mildly baked ($\sim 60^\circ\text{C}$) in the evening after finishing the experiments.

The (001) sample (accuracy $\pm 0.5^\circ$) was clamped to a Ta holder which could mechanically be withdrawn from the liquid- N_2 -cooled manipulator shaft during annealing. In the low-temperature region, the sample temperature was regulated by simultaneous mild heating. The temperature was measured with a Chromel-Constantan thermocouple with an absolute error of about ± 3 K. The relative error when comparing different experimental runs was considerably smaller, about ± 0.5 K. NH_3 coverages will be given in monolayers (ML) referred to unreconstructed Ge(001). 1 ML corresponds thus to an adsorbate density of $6.25 \times 10^{14} \text{ cm}^{-2}$.

III. RESULTS

Figure 1 shows a set of photoelectron spectra taken with $h\nu = 70$ eV during slow cooldown at a constant NH_3 pressure of 2×10^{-8} mbar. The light incidence was at 45° and the escape angle 60° with respect to the sample normal. The spectrum taken at 400 K represents the clean surface. The

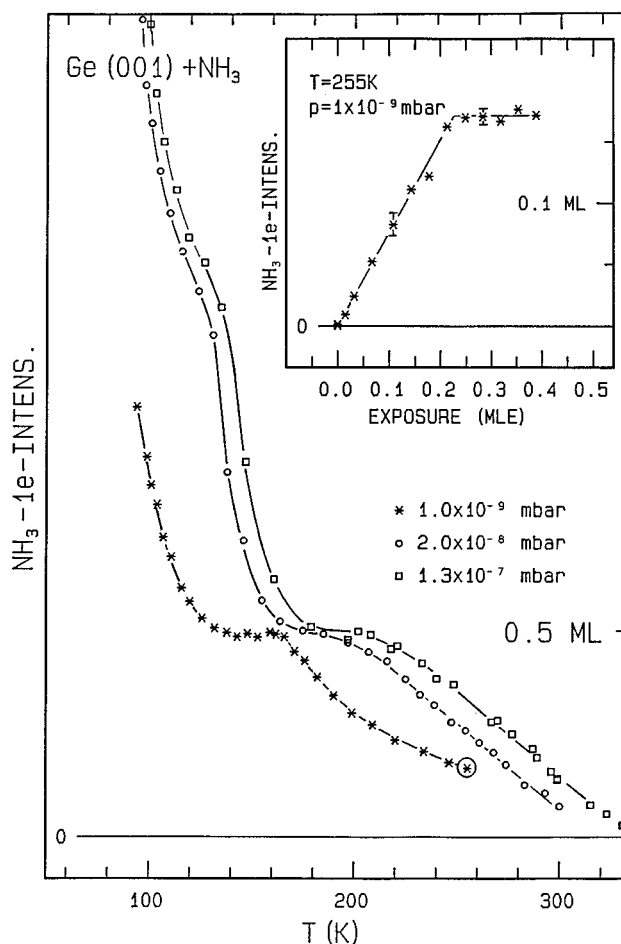


FIG. 2. Dependence of NH_3 coverage in terms of the $1e$ orbital intensity on temperature during slow cooling at the indicated NH_3 pressures. Inset: Dependence of coverage on exposure at 255 K and an NH_3 pressure of 1×10^{-9} mbar. The curve saturates at an equilibrium coverage of 0.17 ML which corresponds to the encircled point in the main figure.

initial α state ($\frac{1}{2}$ ML, completed at 190 K, see Fig. 2), is characterized by the $2a1$ orbital at -23.4 eV, the $1e$ orbital at -11.9 eV, and a weak $3a1$ emission, in complete agreement with previous results.^{5,6,8} With decreasing temperature, the coverage increases and the orbital positions shift to -22.1 eV ($2a1$), -11.1 eV ($1e$), and -5.6 eV ($3a1$) for the spectrum at 100 K representing a coverage of about 2 ML. These values coincide with those reported in Ref. 8 but differ slightly from those in Refs. 5 and 6 which were measured after NH_3 admission at low temperature where the surface mobility is not sufficient to guarantee sequential occupation of the different adsorption states.⁸

The temperature dependence of the NH_3 - $1e$ orbital intensity for three pressures is displayed in Fig. 2. The $1e$ intensities were taken from He I spectra. They are proportional to the coverage Θ_{NH_3} as discussed in more detail elsewhere.⁸ The saturation of the $\frac{1}{2}$ ML state is connected with clear plateaus at about 200 to 150 K, depending on the pressure. The two curves for higher pressures show a further shoulder around 120 K which is connected with the mentioned ΔS transition for $\Theta \approx 1.3$ – 1.5 ML.⁸ For the lowest pressure, the

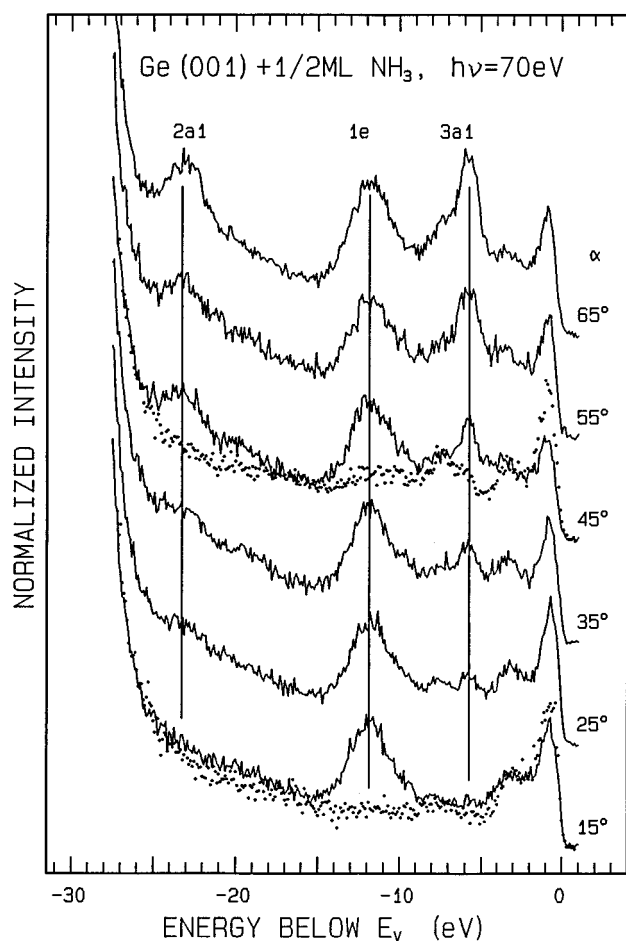


FIG. 3. Photoelectron spectra with $P_{\text{NH}_3} = 2 \times 10^{-8}$ mbar at 190 K in the $\frac{1}{2}$ -ML plateau of Fig. 2. All spectra are taken at normal emission and the incidence angle varied from near normal (15°) to 65° . The dotted spectra are from the clean surface.

coverage did not exceed 1 ML in the attainable temperature range.

The inset shows the coverage increase with exposure time at 1×10^{-9} mbar, expressed in terms of monolayer equivalents (MLE) [1 MLE is the exposure corresponding to the density of surface atoms on Ge(001)] for the first data point at 255 K of the curve below (marked by a circle). The sticking coefficient is constant until saturation at the equilibrium coverage is reached, proving that adsorption occurs via a mobile precursor state. For the applied pressure and temperature, the equilibrium coverage is 0.17 ML. The sticking coefficient turns nominally out as 0.72 but no correction of the pressure reading for the ionization probability of NH₃ has been made and it is likely that the pressure at the sample is lower than at the pressure gauge because of NH₃ pumping by condensation on the cooled sample holder. We can thus say that the sticking coefficient is constant and near unity.

Figure 3 shows 70-eV spectra for $\frac{1}{2}$ -ML saturation (α state) taken for normal emission and variable incidence angle α . The dotted spectra shown for $\alpha = 15^\circ$ and 45° represent clean surface spectra. For 15° (as near to normal incidence as possible), the emission from the orbitals with $a1$ symmetry is almost zero and increases continuously with α . The $1e$ orbital emission is always strong. This is precisely what is to

be expected if the NH₃ molecules are adsorbed perpendicularly, i.e., with the Ge-N axis normal to the surface plane. Only then the $a1$ orbitals cannot be excited with the light polarization vector in the surface plane.^{10,11}

Figures 4(d)–4(f) show schematically possible arrangements of Ge(001) reconstruction dimers and their LEED patterns which consist always of contributions from two rotational domains separated by single-layer steps. The stable low-temperature structure is $c(4 \times 2)$ (Refs. 2, 12, and 13) which is explained by the arrangement of Fig. 4(f). Figure 4(a) shows a pattern measured at 255 K. The $(\frac{1}{2}, \frac{1}{4})$, $(\frac{3}{2}, \frac{3}{4})$, and the corresponding spots from the second domain are elongated [$\sim 3.5\%$ BZ long but only $(0.5\text{--}0.8)\%$ BZ wide; BZ is the Brillouin zone length of the unreconstructed Si(001) surface] indicating oblong domains with a length along the dimer rows of about 500–800 Å and a width of about 120 Å. The order perpendicular to the dimer rows depends on the preparation. In our experiments it decreased from about 7% BZ for the initial sputter-annealed surface to a final value of 3.5% BZ.

At higher temperature, only a 2×1 pattern is observed. Figure 5 illustrates the transition. The quarter-order spots begin to decrease stronger than predicted by the Debye-Waller behavior at about 220 K and have disappeared at about 400 K. This looks very similar to the LEED results of Kevan and Stoffel.¹² In a later paper, however, Kevan gives a quite narrow transition range between about 220 and 250 K deduced from the same LEED data.¹⁴ The whole transition is interpreted as a two-stage process with ordering along the dimer rows as a first and ordering perpendicular to them as a second step. We have no indication for a two-step transition in the investigated temperature range. The ordering along the dimer rows is always quite good (spot width $< 1\%$ BZ) and we did not find stripes along the whole line from $(\frac{1}{2}, 0)$ to $(\frac{1}{2}, 1)$ at higher temperature or any kind of increased background. The $c(4 \times 2)$ -related spots appear during cooling with a width of about 6.5% BZ at 300 K and 3.5% BZ at 250 K.

When NH₃ is adsorbed, the $c(4 \times 2)$ pattern changes very quickly to a 2×2 pattern. Figure 4(b) shows an example. The dependence of this change on exposure is shown in Figs. 6 and 7. Figure 6 shows LEED scans along the line indicated by arrows in Fig. 4(a). The adsorption conditions are similar to those in the inset in Fig. 2 but with lower NH₃ pressure so that the final equilibrium coverage is approximately 0.15 ML. Already for the lowest coverage ($\Theta_{\text{NH}_3} = 0.007$ ML), the quarter-order peaks in Fig. 6 are reduced. For 0.04 ML, only an increased background is left and a clear $(\frac{1}{2}, \frac{1}{2})$ spot has formed which develops further. It has a sharp tip (1.3% BZ) superimposed on a broad base (9% BZ for the 0.07-ML curve) of equal intensity in the maximum. The width of the broad base peak decreases with increasing coverage. The 0.15-ML curve corresponds to equilibrium at the used P_{NH_3} . The two-dimensional pattern of Fig. 4(b) is from this state and shows that the $(\frac{1}{2}, \frac{1}{2})$ spot actually is cross shaped [contour line plot in Fig. 4(c)] which is obviously again due to the contributions from oblong domains from the two unequivalent rotation domains. However, from the LEED pattern alone, it cannot be decided whether they are elongated along or perpendicular to the dimer rows because there exist no spots in the pattern which originate from only one kind of domain as in the case of the $c(4 \times 2)$ structure. From the

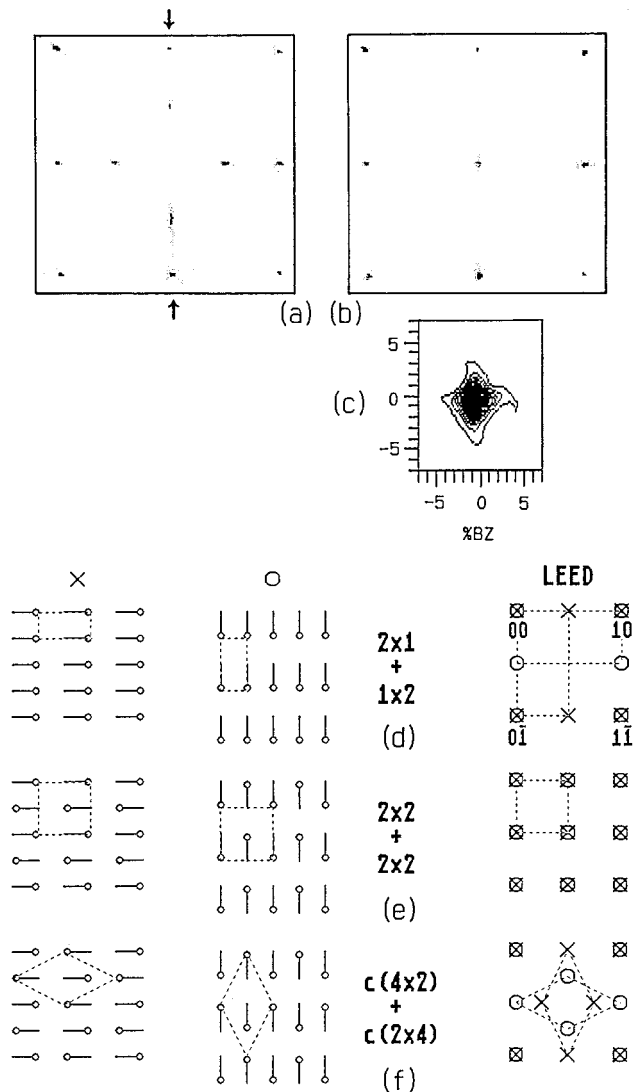


FIG. 4. (a) LEED pattern of the clean Ge(001) $c(4\times 2)$ surface at 255 K, $E_p=120$ eV; shown is a section limited by the integral order spots (00), (10), (0 $\bar{1}$), and (1 $\bar{1}$) as in the schematic patterns below; the arrows indicate the position of the line scans of Fig. 6. (b) Same as (a) but with a constant NH_3 pressure of 5×10^{-10} mbar, $\Theta_{\text{NH}_3}\approx 0.15$ ML; a 2×2 pattern has formed. (c) Contour plot of the central $(\frac{1}{2}, \frac{1}{2})$ spot in (b); scale: 100% BZ corresponds to the (00)-(01) distance in (b). (d) Schematic arrangement of the tilted reconstruction dimers (circles represent up atoms) for two rotational domains of the Ge(001)- 2×1 structure (two further domains with dimers tilted opposite are also possible) and corresponding LEED pattern with the spots from the two domains marked with circles and crosses. (e) Same as (d) for a 2×2 structure. (f) Same as (d) for a $c(4\times 2)$ structure. Representative primitive surface unit cells are marked.

widths of the base and the sharp tip, the dimensions of the formed 2×2 domains can be deduced. Relatively seen, their length varies little with coverage from 280 Å at 0.07 ML to 330 Å at 0.15 ML. Their width, however, varies by more than a factor of 2 from 30 to 65 Å.

Energetically, the difference between the $c(4\times 2)$ and the 2×2 structure is small.^{15,16} The transition from $c(4\times 2)$ to 2×2 requires a dimer flip (change of tilt direction) of every second dimer row in Fig. 4(f). For a complete half ML of

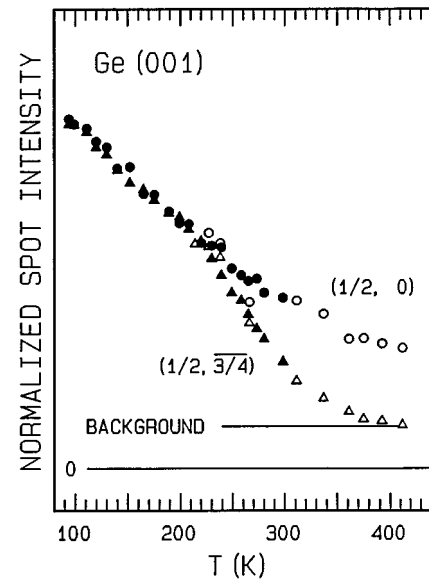


FIG. 5. Temperature dependence of the spot intensity of two reconstruction spots of the clean Ge(001) surface showing the $c(4\times 2)\rightarrow(2\times 1)$ transition around 300 K; $E_p=120$ eV. The intensity of the $(\frac{1}{2}, 0)$ spot follows a Debye-Waller decrease.

NH_3 molecules adsorbed on dimer down atoms, Fig. 8 shows that a 2×2 arrangement might be more favorable than a $c(4\times 2)$ arrangement if a short-range repulsive interaction between adsorbate molecules exists. The 2×2 structure allows for larger distances between NH_3 molecules on neighboring dimer rows. The models in Fig. 8 imply perpendicular adsorption on the dimer down atoms. Perpendicular adsorption results from the photoemission results discussed above. Ad-

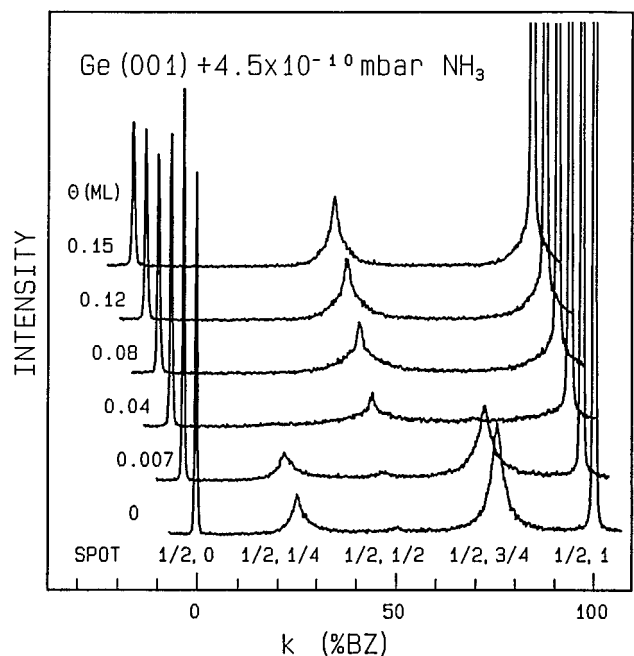


FIG. 6. LEED scans along the line marked by arrows in Fig. 4(a) during NH_3 admission of 4.5×10^{-10} mbar at 255 K; $E_p=120$ eV. The parameter gives the coverage in Ge(001) monolayers. For the top curve, equilibrium coverage is reached.

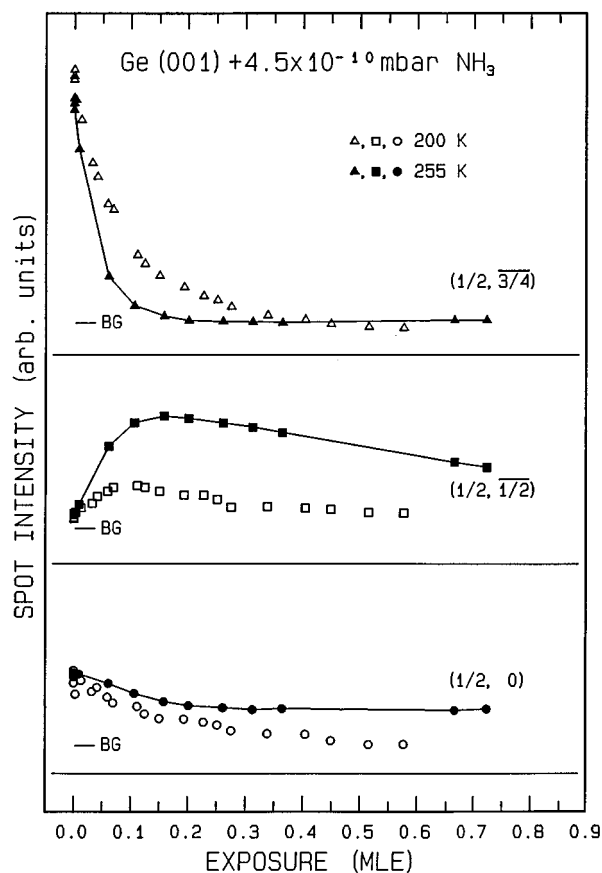


FIG. 7. Dependence of the intensity of the indicated LEED spots from line scans as in Fig. 6 on exposure for a constant NH₃ pressure of 4.5×10^{-10} mbar with the sample at 200 and 255 K. The final equilibrium coverage is approximately 0.25 ML at 200 K and 0.15 ML at 255 K. The background intensity is marked by BG in the curves.

sorption on down atoms was concluded from the behavior of Ge 3d surface core-level shifts on clean and NH₃-covered Ge(001) and their comparison with calculations of Pehlke and Scheffler.¹⁷

However, the adsorbate-induced transition is almost complete after exposure to only about 0.06 MLE ($\Theta_{\text{NH}_3} = 0.04$ ML). Therefore we propose the following mechanism: The NH₃ molecules form islands which kinetically is possible because of the existence of a mobile precursor. A long-range attractive interaction must exist in this case. This seems unlikely for the observed arrangement of parallel strong dipole moments of perpendicularly adsorbed NH₃ molecules. However, we have observed that the heat of adsorption is high and increases with coverage up to $\frac{1}{2}$ ML,⁸ which supports attractive interaction. Further, the strong adsorption-induced work-function decrease of -2.1 eV is strictly linear until $\frac{1}{2}$ -ML saturation without depolarization effects⁸ which supports that repulsion is negligible. A repulsion appears to be restricted to the interaction between dimer rows and causes the 2×2 structure of Fig. 8(a) to be more favorable than the $c(4 \times 2)$ structure of Fig. 8(b). Thus, NH₃-covered 2×2 domains may locally be formed. Since neighboring dimers with the same tilt direction at the island edge are unfavorable, they flip and the 2×2 pattern continues dominolike along the dimer rows resulting in oblong 2×2 domains with their long

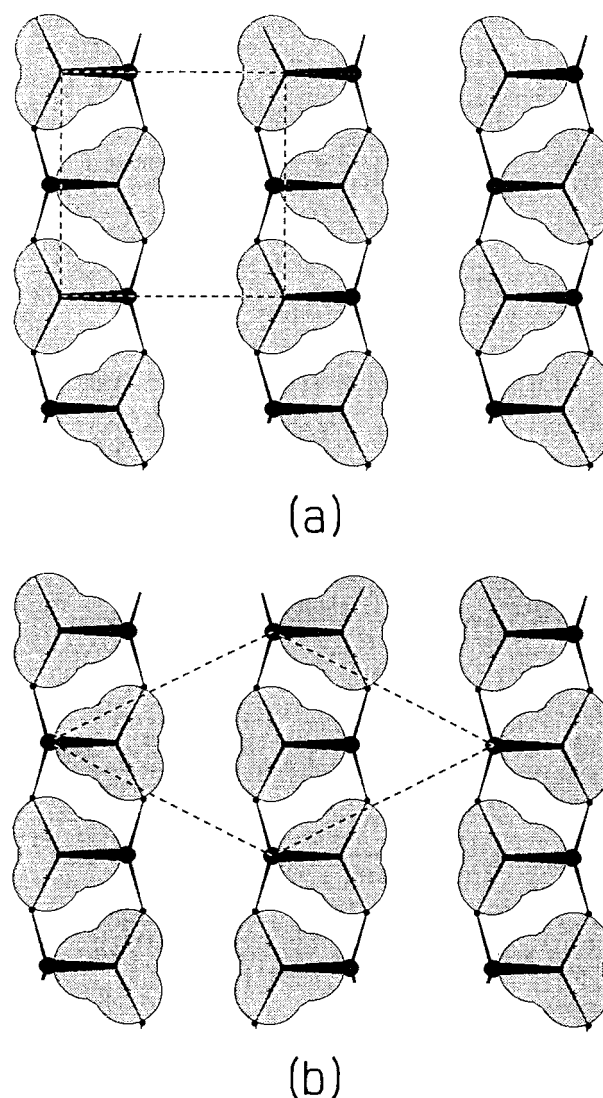


FIG. 8. Structure models for $\frac{1}{2}$ -ML NH₃ adsorbed perpendicular on Ge-dimer down atoms with 2×2 (a) and $c(4 \times 2)$ (b) arrangement. The shaded areas represent the van der Waals radii of H and N atoms in NH₃. The rotational orientation of the molecules is chosen so that the distance between H atoms of different molecules is largest. The distance between H atoms from molecules on neighboring dimer rows is larger for the 2×2 arrangement.

axis along the dimer rows. An exposure to 0.06 MLE ($\Theta_{\text{NH}_3} = 0.04$ ML, less than 10% of the $\frac{1}{2}$ -ML saturation of the α state) is sufficient to transform nearly the whole surface.

One could argue that also random adsorption of NH₃ without island formation could modify the surface energy in a way to let the 2×2 structure be more favorable after having reached a certain sharp value of the coverage. The seeds for 2×2 -domain formation would in that case be fluctuations of the dimer tilt direction, possibly stabilized by single NH₃ molecules, and oblong domains could form similarly by a quick dominolike dimer flip along the dimer rows.

Apart from the fact that the coverage dependence of the heat of adsorption suggests attractive interaction, the coverage-dependent increase of the 2×2 domain width would be hard to explain assuming a phase transition in-

duced by random adsorption. NH_3 island formation could explain it by assuming island growth analogous to Ostwald ripening. The question could be clarified using a real-space microscopic method like scanning tunnel microscopy at low temperature.

The 2×2 pattern after conversion at low NH_3 coverage is dominated by the form factor of the clean surface which then changes towards that of the NH_3 -saturated 2×2 pattern when Θ approaches $\frac{1}{2}$ ML. This behavior is reflected in Fig. 7. The $(\frac{1}{2}, \frac{3}{4})$ spot has reached zero intensity (background intensity) at about 0.1 MLE where the $c(4 \times 2) \rightarrow (2 \times 2)$ transition is completed. The $(\frac{1}{2}, 0)$ spot intensity, however, drops further until about 0.2 MLE where the equilibrium coverage of 0.15 ML is reached.

The $(\frac{1}{2}, \frac{1}{2})$ spot intensity in Fig. 7 increases first, goes through a maximum, and decreases again although the NH_3 coverage no longer changes. We cannot exclude that this is caused by NH_3 decomposition by the continuous electron irradiation over about 35 min giving a dose of about 3×10^{15} electrons per cm^2 . This point was not investigated further. All other spots remain constant after reaching the intensity corresponding to equilibrium coverage.

Figure 7 contains also data for exposure at 200 K. Also here, the intensity of the $(\frac{1}{2}, \frac{3}{4})$ spot drops to the background intensity, but higher exposures (and coverages) are necessary (note that the final equilibrium coverage at 200 K is higher). The $(\frac{1}{2}, \frac{1}{2})$ spot appears also but its intensity remains low. The $(\frac{1}{2}, 0)$ spot decreases continuously. We believe that the tilt of dimer rows connected with the $c(4 \times 2) \rightarrow 2 \times 2$ transition is activated and does therefore not form completely at the lower temperature. The result is much more disorder in the dimer tilt directions. We do not believe that the dimer structure itself is destroyed.

So far, we have only discussed adsorbate-induced changes of the LEED pattern at constant temperature in the range below $\frac{1}{2}$ ML. In order to reach higher coverages, the sample must be cooled further but adsorption at a fixed low temperature implies reduced precursor mobility and inhibited equilibration in the case of activated processes. We have therefore measured the same line scans as in Fig. 6 during slow cooldown at constant NH_3 pressure. The disadvantage is that intensity changes due to the changing Debye-Waller factor have to be considered.

Figure 9 shows the measured dependence of some spot intensities on temperature at constant NH_3 pressure for two representative primary energies. Some NH_3 coverages as deduced from Fig. 2 are also indicated. Already after adjustment of the NH_3 pressure with the sample above 300 K, the few percent of a ML which are on the sample in adsorption-desorption equilibrium are sufficient to change the structure from $c(4 \times 2)$ to 2×2 . Until completion of $\frac{1}{2}$ ML, the intensity of the $(\frac{1}{2}, \frac{1}{2})$ spot [especially at 100 eV, (a)] and thus the 2×2 structure is strong. That it does not show a Debye-Waller-like increase as the $(\frac{1}{2}, \bar{1})$ spot is due to the changing form factor of the 2×2 structure as discussed above when going from the clean-surface dominated structure at low NH_3 coverage to 0.5-ML saturation. Beyond 0.5 ML, the $(\frac{1}{2}, \frac{1}{2})$ intensity drops and becomes diffuse when 1 ML is completed. However, in the whole range down to below 100 K or up to 4 ML, the half-order spot $(\frac{1}{2}, \bar{1})$ remains strong, indicating that the surface, including the NH_3 layer up to about 4 ML, is

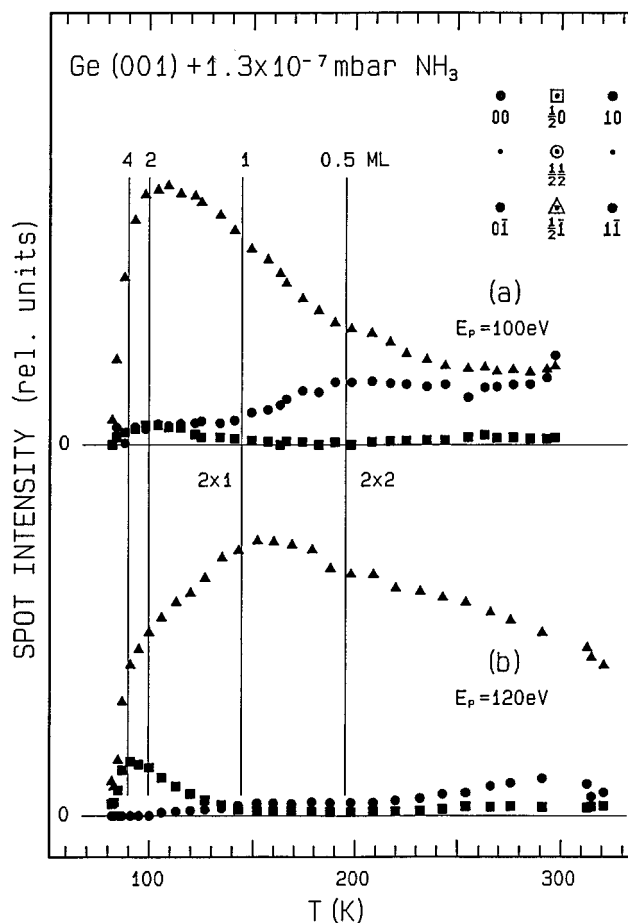


FIG. 9. Intensity variation of three LEED spots marked in the inset by the respective symbols during slow cooldown at constant $P_{\text{NH}_3} = 1.3 \times 10^{-7}$ mbar. Some coverage values as deduced from Fig. 2 are indicated. The primary energy is 100 eV in (a) and 120 eV in (b).

well ordered with a 2×1 structure. The downward break of the $(\frac{1}{2}, \bar{1})$ spot and the simultaneous increase of the $(\frac{1}{2}, 0)$ spot for $E_p = 120$ eV in (b) beyond 1 ML indicate a structural change with changed form factor. This is the coverage region where the ΔS transition was deduced from the $\Theta(T)$ curves (Fig. 2). As shown before,⁸ the work function drops strongly during adsorption of the first half ML with a dipole of 1.8 Debye units per molecule. Beyond $\frac{1}{2}$ ML, the additional dipole is quite small and we have proposed that both upright and inverted molecules are adsorbed at approximately the same rate so that their dipole contribution normal to the surface is canceled. Beyond 4 ML, the whole layer rearranges.⁸ A thick condensed layer is formed and all superstructure spots are quenched. Also the integral order spots become very weak and the background increases. Although the adsorbate structure beyond $\frac{1}{2}$ ML remains speculative, the well-developed 1×2 structure shows that NH_3 grows pseudomorphic up to 4 ML.

IV. CONCLUSIONS

We have shown that the sequence of adsorption states for NH_3 on Ge(001) correlates with a sequence of ordered phases of different periodicity: $c(4 \times 2)$ (clean)

→2×2(α-NH₃, 0.04–0.5 ML)→1×2(β-NH₃, 1–4 ML) →disordered(γ-NH₃, condensed). Especially the first transition $c(4\times 2)$ (clean)→2×2(α-NH₃) is exciting. Photoemission results prove that NH₃ adsorbs with the N end down and the Ge-N bond normal to the surface. At 255 K, the transition to the 2×2 periodicity is completed at a coverage of only 0.04 ML, far below $\frac{1}{2}$ ML saturation. We favor a model implying NH₃ island formation with a local change to 2×2 periodicity due to dimer flip of every second dimer row. This flipping seems to continue dominolike beyond the island

edge so that also the clean parts of the surface convert to 2×2. This behavior is quenched at 200 K which shows that the dimer flip needs thermal activation.

ACKNOWLEDGMENT

The project was supported in part by the Sonderforschungsbereich 296 of the Deutsche Forschungsgemeinschaft.

-
- ¹J. A. Kubby, J. E. Griffith, R. S. Becker, and J. S. Vickers, *Phys. Rev. B* **36**, 6079 (1987).
²M. C. Payne, M. Needels, and J. D. Joannopoulos, *J. Phys. Condens. Matter* **1**, SB63 (1989).
³R. Rossmann, H. L. Meyerheim, V. Jahns, J. Wever, W. Moritz, D. Wolf, D. Dornisch, and H. Schulz, *Surf. Sci.* **279**, 199 (1992).
⁴S. Ferrer, X. Torrelles, V. H. Etgens, H. A. van der Vegt, and P. Fajardo, *Phys. Rev. Lett.* **75**, 1771 (1995).
⁵X. H. Chen and W. Ranke, *Surf. Sci.* **262**, 294 (1992).
⁶W. Ranke and J. Wasserfall, *Surf. Sci.* **303**, 45 (1994).
⁷C. Tindall and J. C. Hemminger, *Surf. Sci.* **330**, 67 (1995).
⁸W. Ranke, *Surf. Sci.* **342**, 281 (1995).
⁹U. Scheithauer, G. Meyer, and M. Henzler, *Surf. Sci.* **178**, 441 (1986).
¹⁰J. Hermanson, *Solid State Commun.* **22**, 9 (1977).
¹¹K. Jacobi, M. Scheffler, K. Kambe, and F. Forstmann, *Solid State Commun.* **22**, 17 (1977).
¹²S. D. Kevan and N. G. Stoffel, *Phys. Rev. Lett.* **53**, 702 (1984).
¹³L. Spiess, A. L. Freeman, and P. Soukassian, *Phys. Rev. B* **50**, 2249 (1994).
¹⁴S. D. Kevan, *Phys. Rev. B* **32**, 2344 (1985).
¹⁵M. Needels, M. C. Payne, and J. D. Joannopoulos, *Phys. Rev. B* **38**, 5546 (1988).
¹⁶H. J. W. Zandvliet, G. P. M. Poppe, C. M. J. Wijers, and A. van Silfhout, *Solid State Commun.* **71**, 63 (1989).
¹⁷E. Pehlke and M. Scheffler, *Phys. Rev. Lett.* **71**, 2338 (1993).